# Matrix Phased Arrays for the Inspection of CFRP-Components

M. Kreutzbruck, D. Brackrock, G. Brekow, H.-J. Montag, R. Boehm, and B. Illerhaus

*BAM Federal Institute for Materials Research and Testing, Unter den Eichen 87; 12205 Berlin Germany*

**Abstract.** Lightweight components are increasingly used in different industrial sectors such as transportation, energy generation and automotive. This growing field includes different types of CFRP-structures, hybrid materials and glued components showing - compared to their pure metallic counterparts- a significant more complicated structure in terms of internal interfaces and anisotropy of material parameters. In this work we present the use of matrix phased array to increase the amount of obtained information to enhance the inspection quality. We used different types of carbon materials such as 6 mm thick uni- and bidirectional prepreg specimens containing impact damages. The latter were introduced with different energy levels ranging from 1.3 to 7.2 J. By scanning a 2.25 MHz matrix array with 6 x 10 elements above the prepreg surface and using different angels of incidence a complete 3D-image was generated which allows the detection of defects as small as 1mm in a depth of 4 mm. A comparison with conventional approaches show that the signal-to-noise ratio can be highly increased. This enables us to visualize the region of damage within the impact zone, clearly showing the cone-like damage distribution along increasing material depth. The detection quality allows the estimation of the opening angles of the cone shaped damage, which can be used for further evaluation and quantitation of energy dependent impact damages.

**Keywords:** Matrix Phased Arrays, Superposition Algorithm, CFRP Materials, Fiber Matrix Structures, Impact Damage
**PACS:** *43.35.Zc, 81.70.Cv

## INTRODUCTION

Unlike metallic materials CFRP exhibits high elastic anisotropy due to the different mechanical properties of the fiber and its orientation. Therefore the sound velocities can vary more than a factor of three depending on the angle between fiber orientation and sound field. Besides the anisotropy CFRP also exhibits a high sound attenuating factor ranging between 10 dB/cm -20 dB/cm for frequencies of 2 MHz. For this reason signals can be very noisy and different of incidence angles should be applied to enhance the statistical basis of the raw data. To non-destructively inspect CFRP-components one usually use computer tomography (CT), ultrasonic testing (UT) and thermographic testing (TT). In some cases also high frequency Eddy current Testing can be very helpful. Relevant CFRP damages and irregularities are delaminations, cracks and porosities and ondulations, respectively. Because of the lightweight material's anisotropy and high scattering effects the early detection of possibly failure relevant defect types is still a challenge. So far easy applicable classical detection methods also do not allow a sure assessment of life time and the development of adequate non-destructive testing techniques are highly desirable.

Non-destructive testing is applied during manufacture for quality control as well as for check-up to detect operational damage. Micro-CT is the technique with highest resolution and significance but it is very complex and costly that it is only used for development purposes and sometimes for random surveillance of manufacture process.

Making use of matrix arrays an ultrasonic testing technique is presented which permits a detailed CFRP damage analysis in contact technique. This technique takes advantage of spatial focusing and two-dimensional angle scans in combination with superposition algorithms for echo signals so that a substantial improvement of resolution and of signal-to-noise can be attained. The anisotropy of CFRP material is considered in case of matrix array control as well as for evaluation of measurement results. Test specimen made of CFRP prepreg plates with uni- and bidirectional directed fiber structures were treated with artificially induced defined impact damage. After this procedure matrix arrays were used for scanning the test specimen in a meandric manner. From the measurement results we reconstructed the corresponding B- and C-scans. Ultrasonic images are compared with the CT results. In the volume under the surface detected depth extension of impact damage is presented in detail for both techniques. Contours of impact damage which can be seen in the ultrasonic image show a context between inserted energy and fiber matrix structure. Ultrasonic analysis thus permits conclusions from inserted impact damage to fiber matrix structure.

*40th Annual Review of Progress in Quantitative Nondestructive Evaluation*
AIP Conf. Proc. 1581, 108-115 (2014); doi: 10.1063/1.4864809

## STATE OF THE ART AND NEW DEVELOPMENTS

Further development of non-destructive testing techniques is particularly promoted by the aircraft industry, because the low weight and the specific insertable high strength properties of carbon reinforced materials offer an essential reduction of fuel costs. Quality control already starts when construction of aircraft components begins. An automated monitoring system is applied to recognize anomalies in the fiber structure of primary CFRP component stages [1]. Lock-in thermography is here suitable for a contactless testing procedure. Surfaces of $1m^2$ can be checked within a few minutes [2]. In case of a detailed analysis and evaluation of small regions of fiber composites computer tomography (CT) offers different possibilities [3].

A large number of elements in the matrix array or 2D array offer a higher flexibility of sound beam control which permits a better resolution in the visualization of results. In recent years these advantages are described in more and more published contributions [4-9]. This also involves imaging algorithms such as SAFT, sampled phased array or more general the full matrix capture method, in which the information of many A-scans from many different transducer positions are combined into C- and B-scans. In this respect Matrix arrays offer innovative application potential for a detailed analysis of carbon fiber reinforced plastics as the noise level generated by the inhomogeneous nature of the specimen can be reduced.

## CFRP TEST MATERIALS

The test specimen consisted of 6 mm thick plates of uni- and bidirectional CFRP with a density of $1.56\ g/cm^3$. The fiber volume was about 55 -60 vol.-% in conjunction with a resin content of 32 -38 %. The specimen material consisting of unidirectional CFRP are manufactured with an upper and lower bidirectional top layer, whereas the specimen material manufactured with a bidirectional layer structure consisted throughout of a 0°/90° layer orientation (see also Table 1).

**TABLE 1.** Material parameters of the two test samples.

| | **Test sample 1** | **Test sample 2** |
|---|---|---|
| Inner layers | Sigrafil CE 1754-600-35 unidirectional prepreg | Sigratex Prepreg CE 8201-245-45S with bidirectional fiber orientation |
| Top and bottom cover layers | Sigratex CE 8201-200-45S | Sigratex Prepreg CE 8201-245-45S |
| Inner layer: 0° - tensile strength | 1550 MPa | |
| Inner layer: tensile elastic modulus | 110 GPa | |
| Inner layer: compression strength | 950 MPa | |
| Laminate thickness | 0.56 mm | 0.25 mm, 0.23 mm |
| fiber volume content | 56 vol.-% | 55 vol. %, 60 vol. % |
| tensile strength | 950 MPa (0°), 900 MPa (90°) | 1100 MPa (0°), 1030 MPa (90°) |
| Bending strength | 1050 MPa (0°), 990 MPa (90°) | 1050 MPa (0°), 990 MPa (90°) |
| Tensile elastic modulus | | 70 GPa (0°), 65 GPa (90°) |

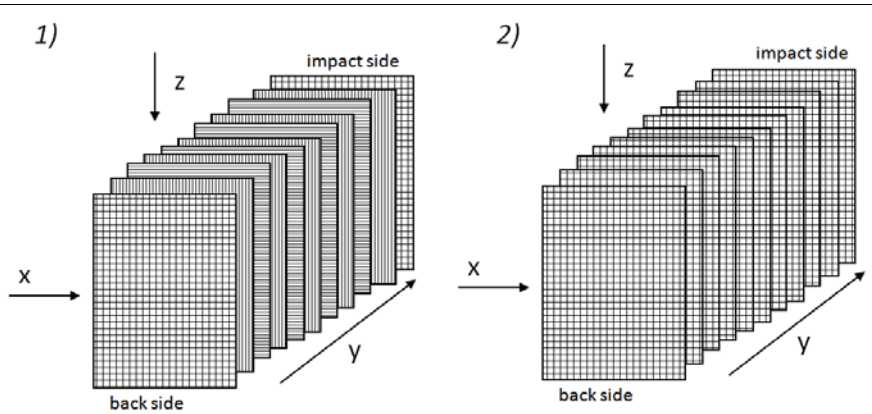


**FIGURE 1.** Fiber layer structures of the tested CFRP materials. Left: sample 1, Right: sample 2.

## ACOUSTIC ANISOTROPY

CFRP materials naturally show a high elastic anisotropy in comparison to metallic materials. Sound velocities of longitudinal waves vary up to a factor of three for propagation directions parallel and perpendicular to the fiber direction. Consequently, anisotropy has to be taken into consideration for the delay time control of matrix arrays. This helps to focus the sound field at certain positions obtaining increased sound energy at the defect.

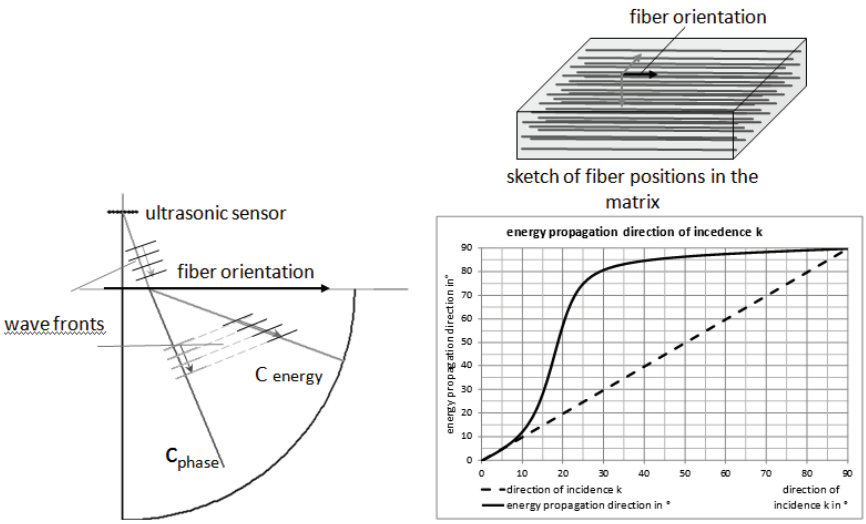


**FIGURE 2.** Acoustical characteristics. Top: fiber orientations within the matrix, bottom Left: Sketch of the deviation mechanism in anisotropic materials. Bottom Right: energy propagation as function of the direction of incidence.

Figure 2 shows differing directions of wave front propagation and of energy propagation which have been calculated from correspondent elastic constants. These calculations are valid for compressive waves in a bidirectional CFRP material. For angles of incidence larger than 10° energy transport mainly occurs in a direction which is close to the fiber direction.

## MEASURING SYSTEM

For preparing detection capabilities of matrix arrays CFRP plates with a thickness of 6 mm has been damaged using an indenter falling down from different drop heights in the range of 1 until 7 m. The indenter has a weight of 670 g.

To analyze the impact damage we used a 2.25 MHz matrix array consisting of 60 transducer elements. Data acquisition occurs on meandric scanning tracks on the specimen surface. The matrix array is connected to the ultrasonic COMPAS device, which is a flexible multichannel UT-hardware and –software platform enabling us to control many emitting and receiving channels simultaneously [10].

Matrix arrays offer the advantage of focusing the sound beam in a two-dimensional area with an orientation in a horizontal, vertical or oblique oriented plane. At the material surface the sound velocity dependent refraction in dependence of the angle of incidence has to be considered. For a given measurement point within the scanning track all single transducer elements are excited according to a delay time distribution which is configured in such a way that the resulting sound pressure is concentrated in a well defined small volume at a given xyz-position. In doing so, for a single transducer position a complete two dimensional focus field is generated consisting of nearby focus points for example covering in our case an area of 15 x 15 mm2. For the evaluation of measurement data a B- or C- scan is then reconstructed taking into consideration echo amplitudes registered at successive measurement points along scanning tracks during measurement. Then all relevant digitized and recorded echo amplitudes of A-scans measured within the focus field are used for the reconstruction of the C-scan.

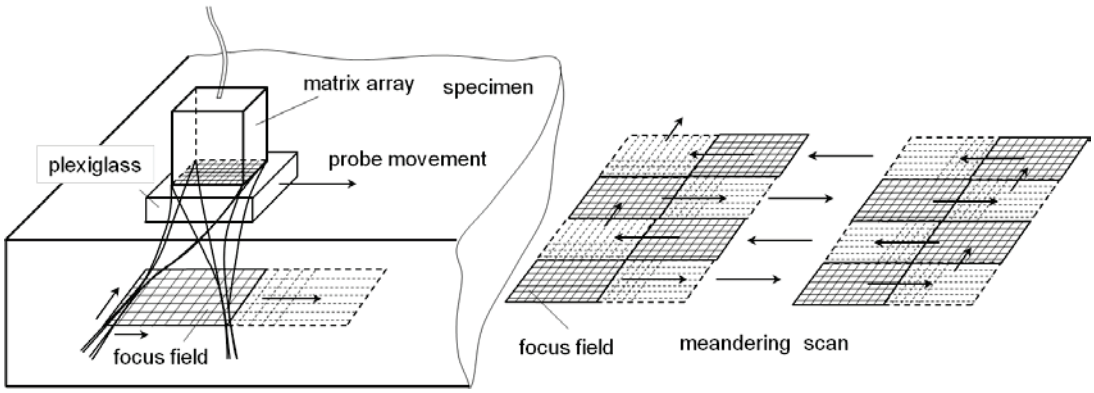


**FIGURE 3.** Schematic overview for data recording using a matrix array.

To obtain the above mentioned C-scan the reconstruction algorithm consists of an echotomographic procedure which can briefly be described as follows: A sum of echo signals coming from spatially related single echoes (A-scans) are received from different sensor positions and from focus spheres round focus points and this sum of echo signals is related to the voxel in the voxel matrix. For the reconstruction algorithm all the position coordinates and the respective time of flights are selected and added, which spatially and temporally could come from the position of the voxel. This is described by a function which in the simplest case can have the value "1" or "0" but can also contain sound field corrections.

The resulting echo signal *VMP* at a single point in the voxel matrix is then composed as follows in equation (1):

$$VMP_{hij} = \sum_{all\ f\ and\ g}^{mechanical\ scan} \sum_{all\ n\ and\ m}^{electronical\ scan} f_{EA}\left(\vec{r}_{VMP}, \vec{r}_{SP}, \vec{r}_{FP}, t\right) \cdot A_{fg\,nm}\left(t\right) \tag{1}$$

whereas the two components in equation (1) are determined by the following definitions (2) and (3):

$$A_{fg\,nm}\left(t\right) = A_{fg\,nm}\left(t\left(\vec{r}_{VMP}(h,i,j), \vec{r}_{SP}(f,g)\right)\right) \text{ and} \tag{2}$$

$$f_{EA}\left(\vec{r}_{VMP}, \vec{r}_{SP}, \vec{r}_{FP}, t\right) = f_{EA}\left(\vec{r}_{VMP}(h,i,j), \vec{r}_{SP}(f,g), \vec{r}_{FP}(n,m), t\left(\vec{r}_{VMP}(h,i,j), \vec{r}_{SP}(f,g)\right)\right) \tag{3}$$

$VMP_{hij}$: scalar pixel value in the voxel matrix

$\vec{r}_{VMP}(h,i,j)$: position of voxel central point

$\vec{r}_{SP}(f,g)$: position of the sensor system

$\vec{r}_{FP}(n,m)$: position of focus point; h, i, j; f, g and n, m are (integer valued) indices

$t\left(\vec{r}_{VMP}, \vec{r}_{SP}\right)$: time of flight of the echo

In the schematic overview in Fig. 3 we show how the focus field is built up to collect echo amplitudes in a certain depth to describe material integrity or inhomogeneity. The matrix array is mounted on a coplanar wedge enabling us to vary the sound beam around the straight beam direction. A hidden defect then can be detected in a certain depth in the inspection volume when the matrix array is moved along a scanning track. Using each voxel element within the focus field and processing all the echo signals coming from neighbored measurement positions as described above we attain an improvement of signal-to-noise ratio and position resolution.

## MEASUREMENT RESULTS

The reconstructed images show the extent and the character of impact damage at CFRP plates created by different drop heights. The CFRP plates were exposed to drop energies between 1.3 and 7.2 J. Figure 4 and 5 represents two results both represented in different viewing direction. We can observe in the B-scan a cone shaped extent of damage in the CFRP material consisting of bi – and unidirectional fiber layers. This is also confirmed by the C-scan, where indications shaped as concentric circles could detected, whose diameter are increased for growing depth. For the double layered CFRP material the cone shaped damage exhibits a large opening angle. For the single layered CFRP material with a throughout bidirectional fiber layer structure the opening angle has a considerable smaller value as shown in Fig. 5.

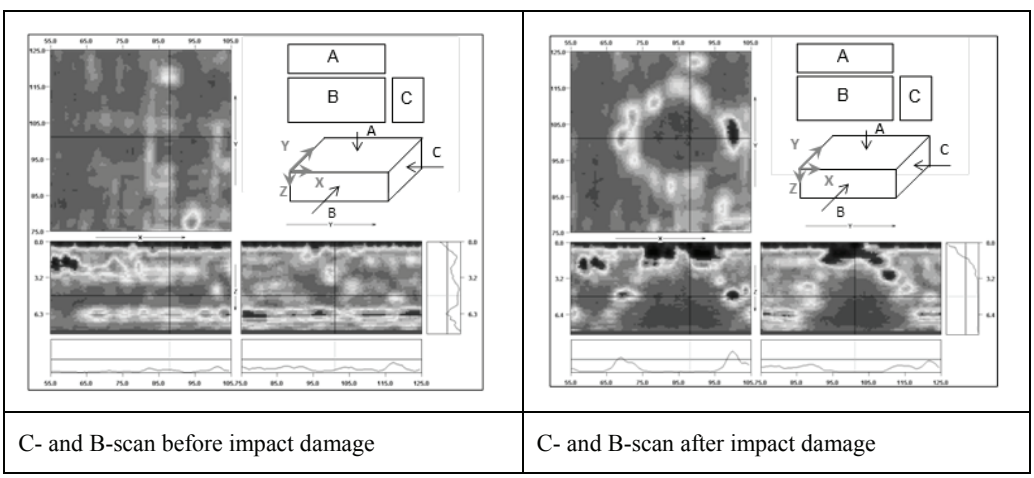


| C- and B-scan before impact damage | C- and B-scan after impact damage |
|---|---|

**FIGURE 4.** Detection of impact damage using a matrix array. Drop height of indenter: 1.1 m, the CFRP-plate consists of bidirectional cover layers and unidirectional inner layers. 1) C-scan representation, 2) B-scan representation, 3) side view of the B-scan representation.

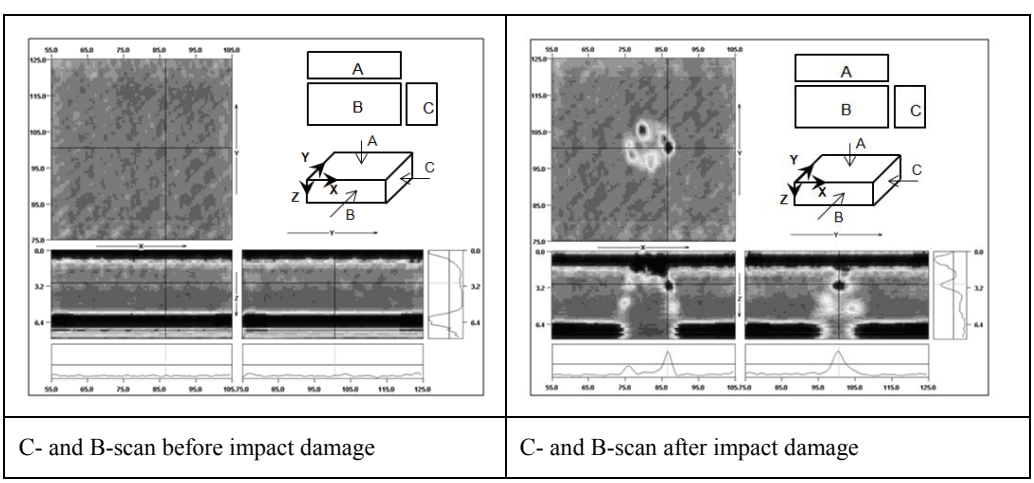


| C- and B-scan before impact damage | C- and B-scan after impact damage |
|---|---|

**FIGURE 5.** Detection of impact damage using a matrix array.
Drop height of indenter: 1.1 m, the CFRP-plate throughout consists of bidirectional fiber layers.
1) C-scan representation, 2) B-scan representation, 3) side view of the B-scan representation.

The delamination characteristics detected by the UT-inspection is confirmed with CT-investigations. We observe in Fig. 6 both interlaminar and intralaminar damage, in which the fiber was separated from the matrix. The distance between the damaged areas from the left area to the right one is also increased for increasing material depth.

In Fig. 7 we plot the drop height of the indenter as function of the opening angles and found a more or less linear behavior for this specific CFRP-plate. From the fracture mechanic field we know that opening angles depend not only on the kinetic energy but also on many more influences such as geometric parameters like size, shape and material of the impactor. We also observed very different angles for different CFRP-specimens depending on their internal structure. For example many different fiber orientations will reduce the resulting cone angle after the damage procedure.

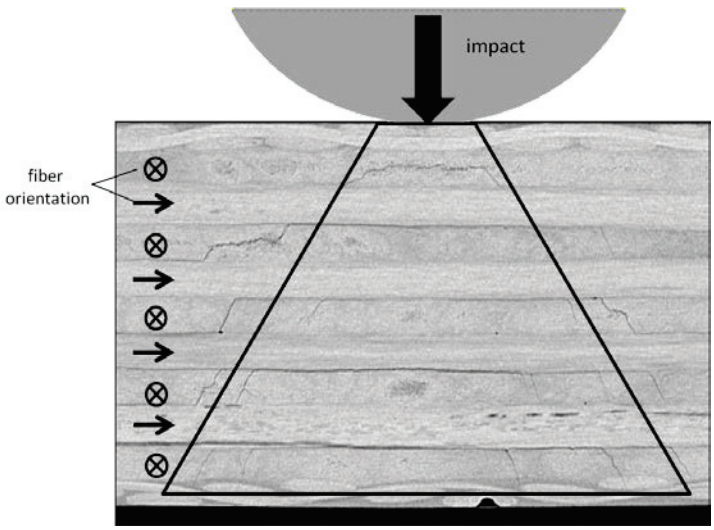


**FIGURE 6.** CT-image of the damaged CFRP material. Black arrows and crosses indicates the fiber orientation and the solid line indicates a roughly estimated area of the cone shaped damage.

In dependence of drop height of indenter the cone shaped damage of CFRP plates is illustrated by different opening angles. Figure 7 represents in a diagram the opening angle γ in dependence of drop height for single and double layered fiber orientations.

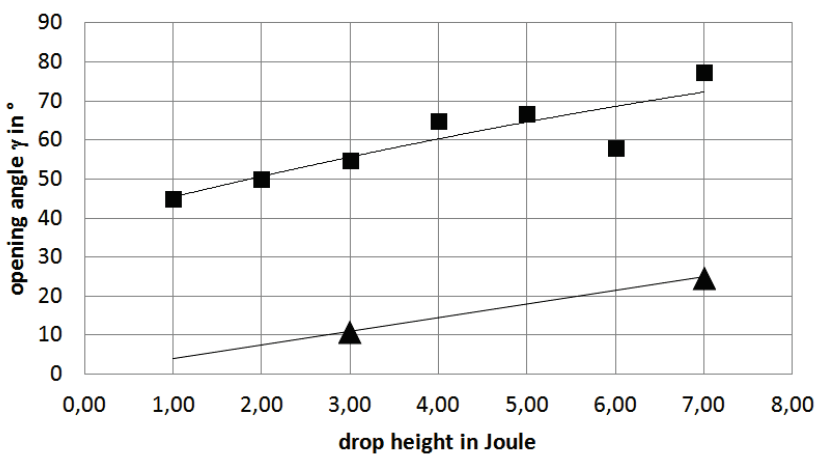


**FIGURE 7.** Opening angle γ as function of the drop height for single and double layered CFRP material.

## DISCUSSION

Impact damage has a typical character of material breakup located on a cone or pyramidal shaped area. The top of the cone is directed to the impact position. In this work we show that the use of a matrix array can help to visualize this cone shaped area. The detection of the cone angle can be very useful from a practical point of view. The matrix UT inspection in its tomographic form can help to identify affected areas which are not visible from outside. This is very important when it comes to decide how much material is removed during the reparation procedure. UT-inspection can be performed very fast and reliable and has therefore many advantages in comparison to radiology based methods.

In case of insonification from the side at which the impactor hits the sample a shadowing effect occurs leading to significantly diminished back wall echo amplitudes. The propagation of delaminations under the surface of the 6 mm thick CFRP plates can only be pursuited by ultrasonic waves penetrating into the volume under the condition of a sufficient position resolution and sensitivity. An ultrasonic testing technique using a straight beam TR probe cannot satisfy the anisotropic property of CFRP material as is shown in Fig. 8. Here we used a reference plate with a thickness of 6 mm containing flat-bottom-holes (FBH) with a diameter of 2 mm and 1 mm. For comparison we used a 2 MHz conventional 0°-probe. We can observe very noisy signals which stem from diffraction effects at the fiber- matrix interfaces (Fig. 8, top, C-scan and B-scan). We also can recognize the superimposed indications of the 2 mm thick FBHs (one in the C-scan and two in the B-scan). In case of the matrix array and the described algorithm we see in Fig. 8, bottom that in contrast to the conventional probe all FBHs can be detected.

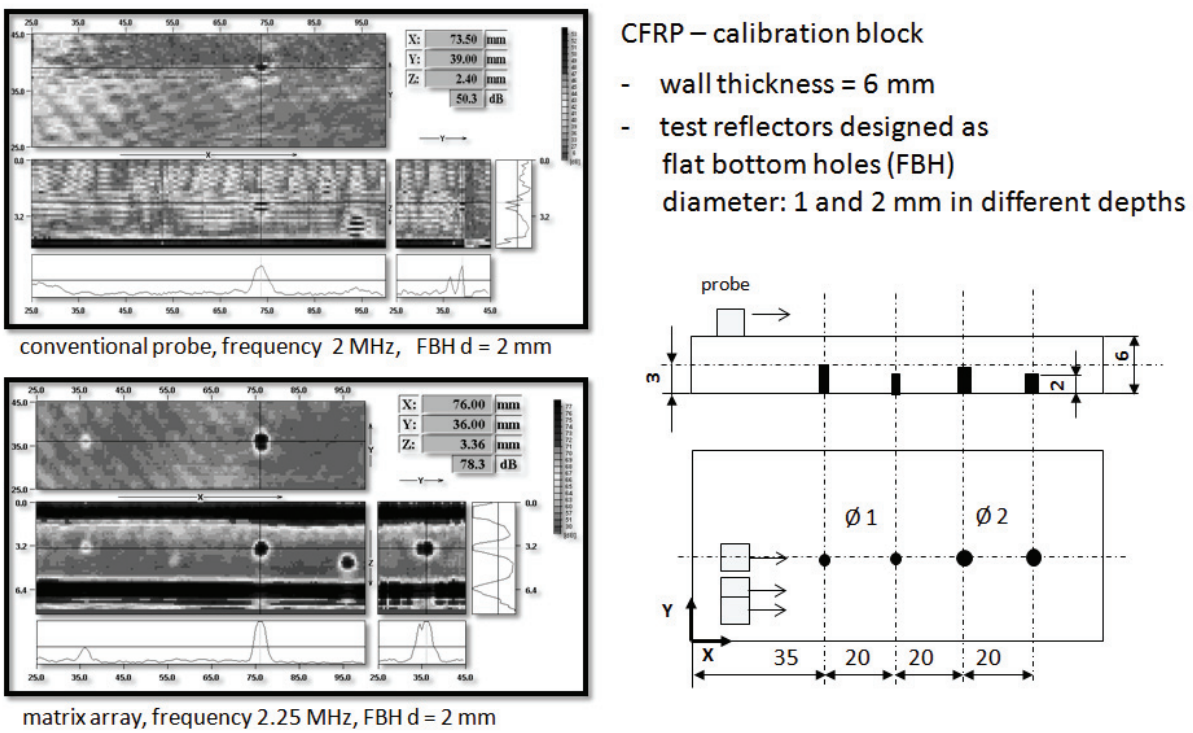


**FIGURE 8.** Left: Comparison of measurement results between matrix array (bottom) and straight beam probe (top), Data are show as C-scan representation (top, left), B-scan representation (middle left), 3) side view of the B-scan representation (middle, right). Additionally line scans are shown for better estimation of the signal-to-noise ratio. Right: Artificial defects implemented into a test plate with throughout bidirectional fiber layer structure. Defect size was 1 mm and 2 mm. The disc shaped reflectors are in a depth of 3 mm and 4 mm.

## SUMMARY

Using matrix arrays in contact technique the anisotropic properties can be taken into consideration by adapting the delay profiles. This helps to form sound fields which are focused at a certain point in the sample volume. Using a very high number of such focused volume points in conjunction with an averaging algorithm makes a detailed damage analysis of CFRP materials possible, as the statistics of the data set is improved. We presented two different types of CFRP plates containing impact damage and a delamination propagation under the surface. The extent is dependent on the fiber layer structure. The observed opening angle of delamination propagation has been detected in comparison to the throughout bidirectional fiber layer structure with an essential larger extent in the case of a CFRP plate with an upper and lower cover layer showing 0/90°- fiber orientation and unidirectional inner layers.

A comparison with conventional transducers shows that in case of matrix arrays a significant increase in signal- to-noise ration can be obtained. Having in mind that smaller matrix arrays can be operated with commercially available UT-devices this technique can easily be used in many applications, when it comes to anisotropic and highly scattering structures. In future work we will address a systematic study, in which we investigate the influence of the number of focus points/ transducer position, the number of matrix elements and the operation frequency on the signal-to-noise ratio and the spatial resolution.

## ACKNOWLEDGMENTS

The authors thank P. Binder from Block Materialprüfungsgesellschaft mbH for preparation of CFRP specimen with impact damage using a drop indenter.

## REFERENCES

1. T. Ullmann, T. Schmidt, S. Hofmann, and R. Jammali, *In-line Quality Assurance for the Manufacturing of Carbon Fiber Reinforced Aircraft Structures*, 2nd International Symposium on NDT in Aerospace 2010-Tu.1.A.4.
2. C. M. Zöcke, *Quantitative Analyse von Defekten in Kompositwerkstoffen mit Hilfe der optischen Lock-in-Thermographie*, Saarbrücker Reihe Materialwissenschaft und Werkstofftechnik / 2010 / 20110205620.
3. U. Hassler, S. Mohr, and A. Müller *Computertomographie zur Analyse von Faserverbundwerkstoffen,* Publisher Name, 1999, Lightweight Design * (2010) Heft 6, **Seite** 35-40.
4. C. Nageswaran, C. R. Bird, and R. Takahashi, *Phased array scanning of artificial and impact damage in carbon fiber reinforced plastic (CFRP)* Insight, Vol.48, No.3, March 2006, pp. 155-159.
5. A. Jüngert, C. Große, MPA Stuttgart, J. Aderhold, P. Meinlschmidt, F. Schlüter, WKI Braunschweig, T. Förster, T. Felsch, N Elkmann, Fraunhofer IFF Magdeburg, M. Krüger, Smartmode, Stuttgart, O. Lutz, Sachverständiger: *Zerstörungsfreie robotergestützte Untersuchung der Rotorblätter von Windenergieanlagen mit Ultraschall und Thermographie* ZfP-Zeitung 115, Juni 2009, S. 43-48.
6. M. Spies, H. Rieder, and E. Rau: *Modell-basierte Optimierung der Ultraschallprüfung anisotroper Werkstoffe am Beispiel von Faserverbundbauteilen*; Fraunhofer Institut für Techno- und Wirtschaftsmathematik ITWM, Cassidian Air Systems; DGZfP-Jahrestagung, Bremen, 30.5.-1.6. 2011.
7. S. Chatillon, S. Mahau, and P. Dubois: *Simulation of Advanced UT Phased Array Techniques with Matrix Probes and Dynamic Settings for Complex Component Inspections*;Rev.of Quantitative Nondestructive Evaluation,Vol. 28,2009, pp. 864-871.
8. S. Chatillon, S. Mahau, and P. Dubois: Simulation of Advanced UT Phased Array Techniques with Matrix Probes and Dynamic Settings for Complex Component Inspections;Rev.of Quantitative Nondestructive Evaluation,Vol. 28,2009, pp. 864-871.
9. C. J. L. Lane, A. K. Dunhill, B. W. Drinkwater, and P. D. Wilcox: The Ultrasonic Measurement of Crystallographic Orientation for Imaging Anisotropic Components with 2D Arrays; Rev. of Progress in Quantitative Nondestructive Evaluation, Vol. 30 (2011) 1335, pp. 803-810.
10. G. Schenk, U. Völz, E. Dohse, BAM Berlin, L. Bauer, MAZ Brandenburg, Werder, COMPAS-XL- outstanding number of channels with a new phased array system, 9th European Conference on NDT, Berlin, 2006-09-25 until 2006-09-29.